

Magnetic Properties of $\text{Sn}_{1-x}\text{Fe}_x\text{O}_2$ Thin Films and Powders Grown by Chemical Solution Method

Yong Hui Li, In-Bo Shim, and Chul Sung Kim*

Department of Physics, Kookmin University, Seoul 136-702, Korea

(Received 15 January 2009, Received in final form 27 November 2009, Accepted 27 November 2009)

Iron-doped $\text{Sn}_{1-x}\text{Fe}_x\text{O}_2$ ($x = 0.0, 0.05, 0.1, 0.2, 0.33$) thin films on Si(100) substrates and powders were prepared by a chemical solution process. The x-ray diffraction (XRD) patterns of the $\text{Sn}_{1-x}\text{Fe}_x\text{O}_2$ thin films and powders showed a polycrystalline rutile tetragonal structure. Thermo gravimetric (TG) - differential thermal analysis (DTA) showed the final weight loss above 430 °C for all powder samples. According to XRD Rietveld refinement of the powders, the lattice parameters and unit cell volume decreased with increasing Fe content. The magnetic properties were characterized using a vibrating sample magnetometer (VSM) and Mössbauer spectroscopy. The thin film samples with $x = 0.1$ and 0.2 showed paramagnetic properties but thin films with $x = 0.33$ exhibited ferromagnetic properties at room temperature. Mössbauer studies revealed the Fe^{3+} valence state in the samples. The ferromagnetism in the samples can be interpreted in terms of the direct ferromagnetic coupling of ferric ions via an electron trapped in a bridging oxygen deficiency, which can be explained using the F -center exchange model.

Keywords : chemical solution method, $\text{Sn}_{1-x}\text{Fe}_x\text{O}_2$, Mössbauer spectroscopy

1. Introduction

Since the discovery of ferromagnetism in Co-doped TiO_2 at room temperature [1], there have been many experimental and theoretical studies on the magnetic properties of transition metal doped semiconductors [2-8]. Understanding the magnetic interactions in a magnetic semiconductor has been a subject of intensive research, which has greatly enhanced our basic knowledge of magnetism. Many theories have been proposed and this subject is still a matter of controversy. This study is an experimental investigation into the effects of iron doping above 5% on the structural and magnetic properties of tin oxide (SnO_2). Among the various transition metal additives, Fe is of particular interest because the ferromagnetism in Fe-doped SnO_2 was proposed from a F -center exchange model [9, 10]. Fe-doped SnO_2 is considered a promising material for the development of multifunctional magnetooptoelectronic devices.

2. Experimental

Iron-doped $\text{Sn}_{1-x}\text{Fe}_x\text{O}_2$ ($x = 0.0, 0.05, 0.1, 0.2, 0.33$) thin films and powders were fabricated by a chemical solution method. Weighed amounts of tin acetate ($\text{Sn}(\text{CH}_3\text{CO}_2)_4$) and iron nitrate nonahydrate ($\text{Fe}(\text{NO}_3)_3 \cdot 9\text{H}_2\text{O}$) were first dissolved in 2-methoxyethanol, acetic acid, diethanolamine, and distilled water. The solution was heated under reflux at 80 °C for 12 h to allow gel formation. Before film deposition, the Si (100) substrates were cleaned with acetone and methanol in an ultrasonic bath. The films were deposited at 600 rpm for 4 s and 3000 rpm for 15 s by spin-coating. They were then pyrolyzed on a hot plate at 80 and at 250 °C for 3 min between each coating step to increase the layer thickness. For the powder samples, the solutions were dried at 120 °C for 48 h. Thermo gravimetric (TG) - differential thermal analysis (DTA) were carried out on the powders xerogel up to 1000 °C at a heating rate of 5 °C/min to determine the crystallizing temperature. The compositions of all powder and thin film samples were annealed at 800 °C. In particular, the thin film samples with $x = 0.33$ were annealed at various temperatures (300, 400, 500, 600, 700, 800, and 900 °C) to allow the formation of the highly homogeneous developed phase. The crystal structure of the samples was

*Corresponding author: Tel: +82-2-910-4752
Fax: +82-2-910-5170, e-mail: cskim@kookmin.ac.kr

examined by x-ray diffraction (XRD) with Cu K_α ($\lambda = 1.54056 \text{ \AA}$) radiation. The thickness of the prepared thin film was measured by field emission scanning electron microscopy (FE-SEM). The magnetic properties were characterized using a vibrating sample magnetometer (VSM) and Mössbauer spectroscopy. In the thin film magnetization measurements, the magnetic field was applied parallel to the sample plane. The Mössbauer spectra were recorded using an electromechanical type spectrometer with a ^{57}Co source in a rhodium matrix.

3. Results and Discussion

TG and DTA were carried out on the powder xerogel up to 1000°C at a heating rate of $5^\circ\text{C}/\text{min}$. The weight losses on the TG curves and the corresponding endothermic peaks on the DTA curves were attributed to the decomposition of the organic compound in the compositions. Fig. 1 shows the TG and DTA plots of the dried $\text{Sn}_{1-x}\text{Fe}_x\text{O}_2$ ($x = 0.0, 0.1$) gel powder compositions. As expected, the decomposition reaction was strongly exothermic. The exothermic peak at 265°C and 269°C for $x = 0.0$ and 0.1 , respectively, was relatively sharp and intense. The weight change associated with this exothermic reaction was approximately 26% and 33% for $x = 0.0$ and 0.1 , respectively. The sharp exothermic peak with a rapid weight drop was attributed to decomposition of the mixed solvent and the evaporation of metal salts and/or decomposition of a by-product. Figs. 2 and 3 show the x-ray diffraction patterns of $\text{Sn}_{1-x}\text{Fe}_x\text{O}_2$ ($x = 0.0, 0.05, 0.1, 0.2, 0.33$) thin

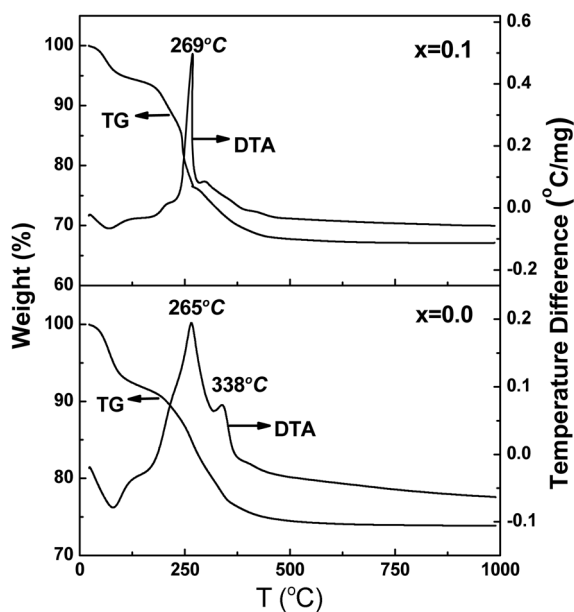


Fig. 1. The TG and DTA plots of the dried $\text{Sn}_{1-x}\text{Fe}_x\text{O}_2$ ($x = 0.0, 0.1$) gel powders.

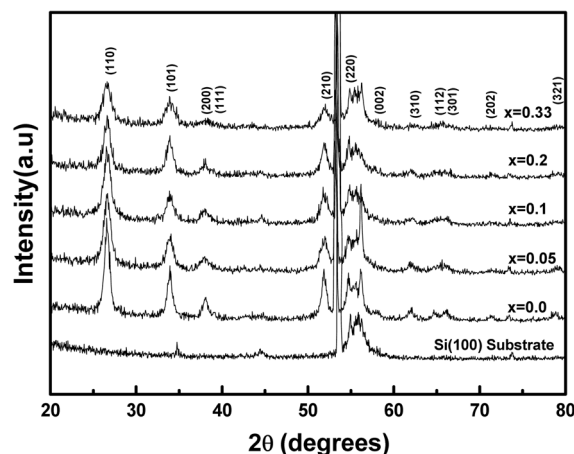


Fig. 2. The x-ray diffraction patterns of $\text{Sn}_{1-x}\text{Fe}_x\text{O}_2$ ($x = 0.0, 0.05, 0.1, 0.2$ and 0.33) thin films and Si(100) substrate at room temperature.

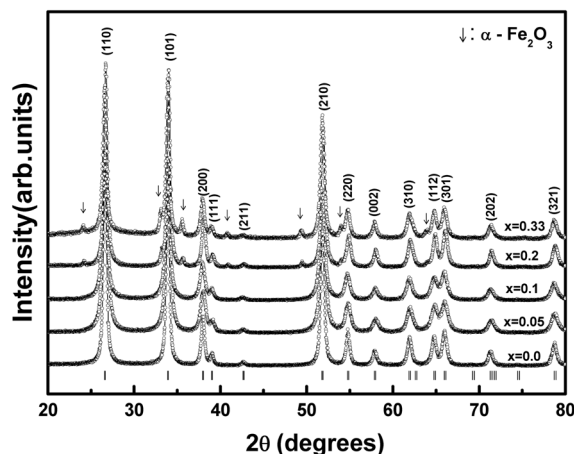
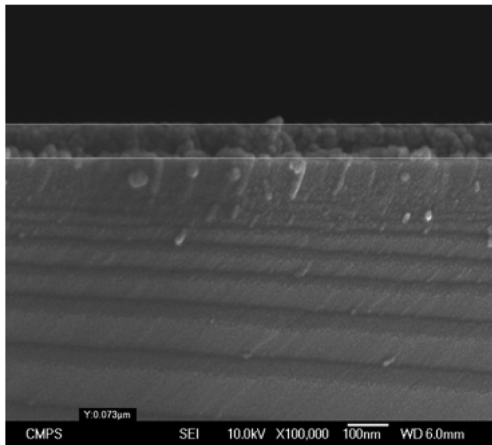


Fig. 3. The x-ray refinement of $\text{Sn}_{1-x}\text{Fe}_x\text{O}_2$ ($x = 0.0, 0.05, 0.1, 0.2$ and 0.33) powders at room temperature.

films and powders ($x = 0.0, 0.05, 0.1, 0.2, 0.33$), respectively. In Fig. 2, the XRD patterns of the Fe-doped SnO_2 films showed a polycrystalline single phase without any Fe related crystallites due to segregation. All the diffraction patterns were assigned to the tetragonal rutile phases of tin oxide (SnO_2). Although the XRD patterns of the SnO_2 thin films with a Fe concentration up to $x = 0.33$ showed a single phase, the XRD patterns for $x = 0.2$ and 0.33 indicated the coexistence of rutile $\text{Sn}(\text{Fe})\text{O}_2$ and $\alpha\text{-Fe}_2\text{O}_3$ phase. In order to examine the changes in the detailed local structure, a Rietveld refinement was performed for $x = 0.0, 0.05$, and 0.1 powder XRD patterns. The crystal structure of the powder samples was determined to be a tetragonal structure with the space group $P4_2/mnm$ by Rietveld refinement, and the final Bragg factors, R_B and R_F , for all patterns were $< 3\%$. With increasing Fe concentration from $x = 0.0$ to 0.1 , the lattice

Table 1. Summary of the $\text{Sn}_{1-x}\text{Fe}_x\text{O}_2$ powders from XRD Rietveld refinement analysis; The synthesis parameters, lattice constant, lattice volume, Bragg factors (R_B , R_F), and oxygen deficiency.

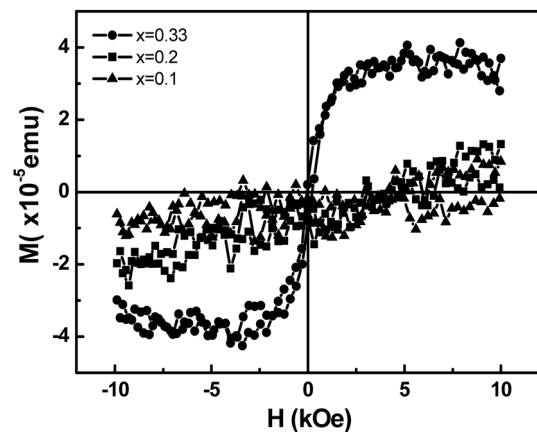
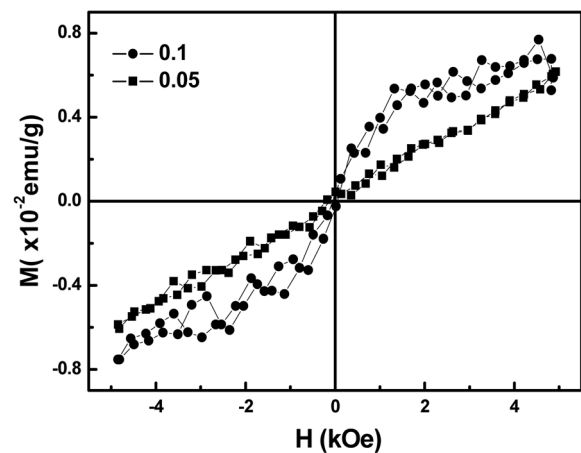
Fe content (x)	lattice constant (Å)		lattice volume (Å^3) V	R_B %	R_F %	oxygen deficiency %
	a_0	c_0				
0.0	4.7400	3.1871	71.6058	2.98	2.16	6.8
0.05	4.7388	3.1851	71.5389	2.22	1.47	8.7
0.1	4.7380 (± 0.0001)	3.1836 (± 0.0001)	71.4679 (± 0.0001)	1.24 (± 0.01)	1.97 (± 0.01)	12.8 (± 0.1)

**Fig. 4.** FE-SEM images of $\text{Sn}_{0.67}\text{Fe}_{0.33}\text{O}_2$ thin film on Si (100) substrate.

constant a_0 decreased from 4.7400 to 4.7380 ± 0.0001 Å, and c_0 decreased from 3.1871 to 3.1836 ± 0.0001 Å. In addition, the unit cell volume decreased with increasing Fe concentration. Table 1 lists the refined parameters. This can be explained by the difference in ionic radii, $\text{Fe}^{3+} = 0.69$ Å and $\text{Sn}^{4+} = 0.83$ Å. From the Rietveld refinement of the powder XRD patterns, the oxygen deficiency concentration for Fe-doped SnO_2 increased with increasing Fe concentration.

Fig. 4 shows FE-SEM images of $\text{Sn}_{0.67}\text{Fe}_{0.33}\text{O}_2$ thin films on the Si (100) substrate. The thickness of the $\text{Sn}_{0.67}\text{Fe}_{0.33}\text{O}_2$ thin film was determined to be 73 nm. This suggests that $\text{Sn}_{1-x}\text{Fe}_x\text{O}_2$ ($x = 0.0, 0.05, 0.1$, and 0.2) thin film samples have similar thickness due to the same preparation conditions.

The magnetic properties were characterized by VSM and Mössbauer spectroscopy. Fig. 5 shows the magnetization curves at room temperature for the Fe-doped SnO_2 thin films. As shown in Fig. 5, the ferromagnetic properties of the $\text{Sn}_{0.67}\text{Fe}_{0.33}\text{O}_2$ thin film revealed a coercivity of 137 Oe at room temperature. With the exception of the $\text{Sn}_{0.67}\text{Fe}_{0.33}\text{O}_2$ thin film, all thin films showed paramagnetic behavior. In the case of powder samples, the $x = 0.05$ sample showed the paramagnetic behavior, which is in contrast to the weak ferromagnetic behavior observed

**Fig. 5.** Magnetic hysteresis loops at room temperature for $\text{Sn}_{1-x}\text{Fe}_x\text{O}_2$ ($x = 0.1, 0.2, 0.33$) thin films.**Fig. 6.** Magnetic hysteresis loops at room temperature for $\text{Sn}_{1-x}\text{Fe}_x\text{O}_2$ ($x = 0.05, 0.01$) powders.

for the $x = 0.1$ sample, as shown in Fig. 6.

The origin of the magnetism in the Fe doped SnO_2 is believed to be a F -center exchange ($\text{Fe}^{3+} - \text{vacancy} - \text{Fe}^{3+}$) model [9, 11]. In a recent paper, Coey *et al.* proposed a ferromagnetic exchange mechanism involving oxygen vacancies (\square), which form F -centers with trapped electrons, for the observed ferromagnetism in the Fe-doped SnO_2 thin films. The VSM measurements of this $\text{Sn}_{1-x}\text{Fe}_x\text{O}_2$ sample suggests that the ferromagnetic behavior of

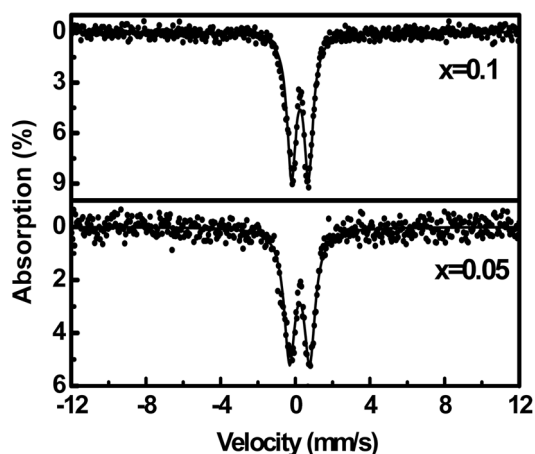


Fig. 7. The Mössbauer spectra of $\text{Sn}_{1-x}\text{Fe}_x\text{O}_2$ ($x = 0.05, 0.1$) powders taken at room temperature.

the $x = 0.33$ doped thin film and $x = 0.1$ powder samples follow the F -center exchange model, according to the increasing oxygen deficiency from 6.8% to 12.8% with increasing dopant concentration from $x = 0.0$ to $x = 0.1$ using a Rietveld refinement, as summarized in Table 1.

Fig. 7 shows the Mössbauer spectra of the $\text{Sn}_{1-x}\text{Fe}_x\text{O}_2$ ($x = 0.05$ and 0.1) powders taken at room temperature. The spectrum displayed a single doublet with electric quadrupole splitting (ΔE_Q) of 1.07 mm/s for $x = 0.05$ and 0.91 mm/s for $x = 0.1$. The isomer shift (δ) of the doublet for $x = 0.05$ and 0.1 was found to be 0.23 and 0.25 mm/s relative to Fe metal, respectively, which is consistent with the Fe^{3+} charge state [12, 13]. The Fe^{3+} ions constituting this doublet are located at the Sn^{4+} sites, which indicate that the oxygen deficiency is caused by Fe^{3+} ions.

4. Conclusion

Iron-doped $\text{Sn}_{1-x}\text{Fe}_x\text{O}_2$ ($x = 0.0, 0.05, 0.1, 0.2,$ and 0.33) thin films and powders are fabricated by a chemical solution method. The prepared samples with a Fe-doping concentration varying from 0 to 33% showed a rutile tetragonal structure. XRD refinement analysis showed that the lattice parameters and cell volume decreased with increasing Fe content, and indicated the presence of oxygen deficiencies in the samples. Ferromagnetic behavior at room temperature was observed for the $x = 0.33$ thin

film and $x = 0.1$ powder samples. On the other hand, paramagnetic behavior was observed in the other thin film and powder samples. The Mössbauer spectra showed that the iron was mainly in the form of Fe^{3+} , which substituted for the Sn^{4+} sites. This can be direct evidence of oxygen deficiencies caused by presence of Fe^{3+} ions in place of Sn^{4+} , which in turn leads to the ferromagnetic behavior.

Acknowledgment

This study was supported by Basic Science Research Program through the National Research Foundation of Korea (NRF) grant funded by the Korea government (MEST) (2009-0083645).

References

- [1] Y. Matsumoto, M. Murakami, T. Shono, and T. Hasegawa, *Science* **291**, 854 (2001).
- [2] K. J. Kim, Y. R. Park, G. Y. Ahn, and C. S. Kim, *J. Magnetism* **11**, 12 (2006).
- [3] D. Karmakar, S. K. Mandal, R. M. Kadam, P. L. Paulose, A. K. Rajarajan, T. K. Nath, A. K. Das, I. Dasgupta, and G. P. Das, *Phys. Rev. B* **75**, 144404 (2007).
- [4] W. Wang, Z. Wang, Y. Hong, J. Tang, and M. Yu, *J. Appl. Phys.* **99**, 08M115 (2006).
- [5] K. Nomura, C. A. Barrero, J. Sakuma, and M. Takeda, *Phys. Rev. B* **75**, 184411 (2007).
- [6] A. Punnoose, J. Hats, V. Gopal, and V. Shutthanandan, *Appl. Phys. Lett.* **85**, 1559 (2004).
- [7] H. M. Lee and C. S. Kim, *J. Appl. Phys.* **101**, 09H110 (2007).
- [8] J. F. Liu, M. F. Nu, P. Chai, L. Fu, Z. L. Wang, X. Q. Cao, and J. Meng, *J. Magn. Magn. Mater.* **317**, 1 (2007).
- [9] J. M. D. Coey, A. P. Douvalis, C. F. Fitzgerald, and M. Venkatesan, *Appl. Phys. Lett.* **84**, 1322 (2004).
- [10] R. Adhikari, A. K. Das, D. Karmakar, T. V. Chandrasekhar Rao, and J. Ghatak, *Phys. Rev. B* **78**, 024404 (2008).
- [11] A. Punnoose, J. Hys, A. Thurber, M. H. Engelhard, R. K. Kukkadapu, C. Wang, V. Shutthanandan, and S. Thevuthasan, *Phys. Rev. B* **72**, 054402 (2008).
- [12] S. I. Park, K. R. Choi, T. Kouh, and C. S. Kim, *J. Magnetism* **12**, 137 (2007).
- [13] K. Nomura, C. A. Barrero, J. Sakuma, and M. Takeda, *Phys. Rev. B* **77**, 184411 (2007).